

Parametric Study of EAA Polymer Thin Film Deposition on Carbon Substrates in a Fluidized Electrode Bed Reactor

V. M. DESAI,¹ R. MAHALINGAM,^{1,*} and R. V. SUBRAMANIAN²

Departments of ¹Chemical Engineering and ²Mechanical & Materials Engineering, Washington State University, Pullman, Washington 99164-2710

SYNOPSIS

Electrodeposition of ethylene-*co*-acrylic acid (EAA) polymer, as thin films on carbon particle substrates, was carried out in a fluidized electrode bed reactor. Feeder current, time of deposition, and flow rate of anolyte (i.e., bed expansion or bed porosity) were the key parameters investigated. The film characteristics were evaluated through SEM and FTIR analyses and the amounts determined by weighing. The effect of these parameters on the electrodeposition process is discussed, and optimum conditions for deposition are proposed. Also, a possible mechanism for electrodeposition, particularly for the EAA-carbon system, is discussed.

INTRODUCTION

Electrode reactions are traditionally carried out in stationary cells for metals recovery. In our work, electropolymerization is investigated in a fluidized electrode bed reactor (FEBR). FEBR gives the following important advantages over a stationary cell:

1. High mass transfer rates due to the continuous disturbance of the diffusion boundary layer caused by particle collisions and turbulence;
2. Low current densities favorable for electroorganic reactions;
3. Large electrode surface area per unit electrode volume; and
4. Uniform coating of film on the surface.

Teng¹⁻⁴ studied the electropolymerization of nonconductive films of polyacrylic acid (PAA), polydiacetone acrylamide (PDAA), and polyacrylonitrile (PAN) on highly conductive metal particle substrates in an FEBR. This work was extended by Segelke et al.^{5,6} for the electropolymerization of conductive polymer films of polyaniline (PA) on conductive graphite particle substrates. The present work evaluates electrodeposition of nonconductive copolymer films on these graphite particles. The co-

polymer chosen for the study was ethylene-*co*-acrylic acid (EAA).

EXPERIMENTAL METHODOLOGY

Materials Preparation

The experiments used a bed of graphite particles as the working electrode, the anode. A bandsaw was used to cut cylindrical particles out of 3.2 mm ($\frac{1}{8}$ in.) diameter machined graphite rods (National Electrical Carbon Corp.). The graphite had a density of 1.8 g/mL and a specific resistance of 10 ohm-meters. The average length of the particles was 4 mm, as determined with a micrometer. The average surface area of the particles was found to be 7.52 sq cm/g. An uncut graphite rod was used as the current feeder. It was coated, except for the ends, with polyurethane in order to render its surface nonconductive. Such a coating left only 1.9 sq cm of the rod surface at its immersed end as the electrically active area.

EAA copolymer solution used was supplied by Dow, had a density of 0.96, and molecular weight of 6000 and consisted of 33.5% by weight of EAA. The EAA consisted of 20% acrylic acid and 80% ethylene.

Experimental Setup

The FEBR was a concentric cylindrical dual compartment cell made of polysulfone with the central

* To whom correspondence should be addressed.

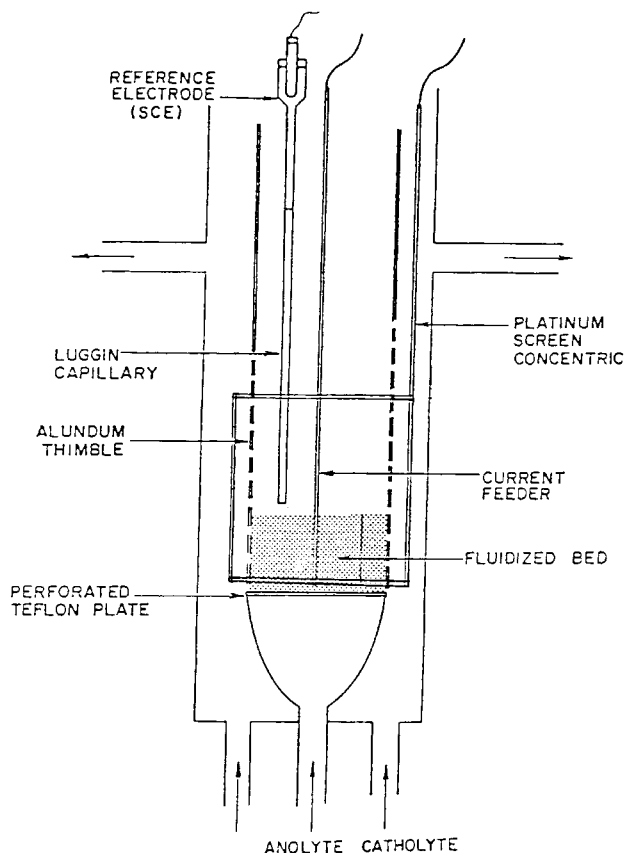


Figure 1 Fluidized bed electrode details.

compartment used as the anodic and the outer compartment as the cathodic compartment, as shown in Figure 1. The compartments were separated by

an alundum thimble, and a perforated Teflon plate was used to support the bed of particles as well as to serve as a flow distributor. The reactor was 280 mm (11 in.) tall with an external diameter of 86 mm (3 3/8 in.). The internal diameter of the central anodic compartment was 40 mm (1 9/16 in.).

The cathode was a cylindrical platinum screen placed inside the cathode compartment. The anode was a bed of cylindrical graphite particles weighing about 10 g dumped inside the anode compartment. Current was fed to the particles through the current feeder, described previously. Electrical power was supplied by a power supply unit from Systron-Donner Corp., Model RS 320-2C, and had a rating of 0-320 V DC/2A. The voltage measurements were monitored manually every 30 s on a voltmeter.

The flow diagram is shown in Figure 2. The solution used in each of the compartments was circulated by corrosion-resistant pumps through flow meters and stainless steel valves. The pump used for anolyte circulation was manufactured by Sethco Division of Met Pro Co., Model PM-1/6EF, and had a 1/2 hp motor. The pump for catholyte circulation was from Little Giant Pump Co., Model 3-MD-MT-HC.

Experimental Runs

The experiments were performed at a constant feeder current. The parameters studied were feeder current, time of deposition, and flow rate of anolyte EAA solution. Both the anolyte and catholyte were 2000 mL of the same EAA solution maintained at

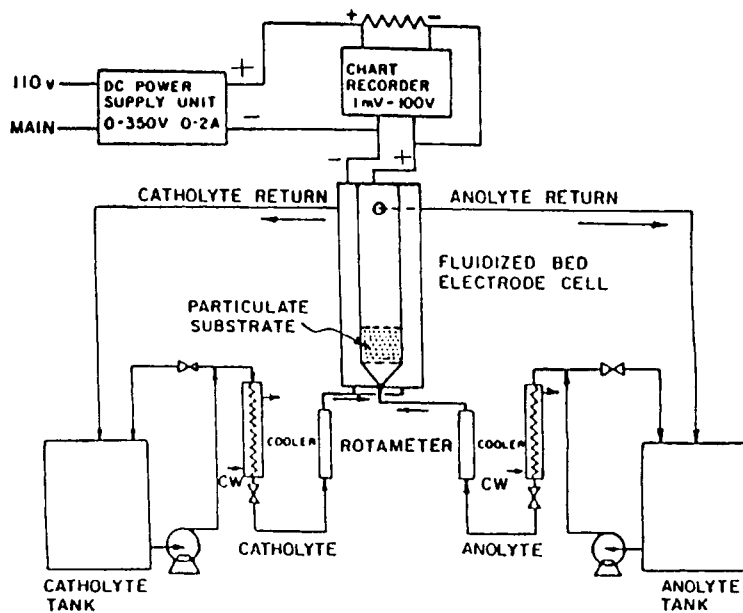


Figure 2 Flow diagram.

the same concentration of 5 wt % and same pH of 9.2 for all the experiments. The EAA solution was prepared by diluting the 33.5 wt % EAA solution with appropriate amounts of water while constantly heating and stirring the solution with a magnetic heater and stirrer assembly. The pH adjustment was by addition of ammonium hydroxide.

The first parameter investigated was the feeder current. The feeder current was varied from 0.05 to 0.25 amp. The time of deposition feasible and amount of deposition obtained were recorded for each experiment. A bed expansion of 22.2% was used in each case. This bed expansion value was selected as the optimum based on work done previously by Teng¹ on electropolymerization in an FEBR.

Next, the effect of deposition time on polymer deposition was investigated. The time was varied from 1 min to a maximum of 3 min. This also was done at a bed expansion of 22.2%. The feeder current was maintained constant at 0.2 amp for each experiment.

Finally, the effect of anolyte flow rate (i.e., effect of bed expansion or bed porosity) on polymer deposition was investigated. Experiments were carried out for no-flow condition (i.e., stationary bed) and also for flow rate variations from 10 to 31.25 mL/s. Incipient fluidization was observed at 16.7 mL/s. These experiments were carried out at a 0.2 amp feeder current and for a deposition period of 3 min.

Evaluation of Polymer Deposits

The amount of polymer deposited was measured by weighing the particles before and after deposition. The dry graphite particles were weighed out into approximately 10 g samples and their precise weight

recorded. After the particles had been coated with the polymer, they were first washed thrice with water to remove the excess solution and then heated in an oven to a temperature of 60°C, for about 15 min, and the weight of the dry polymer-coated particle was determined. Subtracting the coated weight from the initial weight yielded the weight of the polymer deposited. The same weighing procedure was followed for the deposit on the graphite current feeder.

A scanning electron microscope was used to study changes in both thickness and surface morphology by examining a representative particle from each experimental run. The coated particles were glued to aluminum SEM mounts with epoxy and then sputter-coated with gold. An Hitachi S-570 electron microscope was then used to examine the samples. Representative photographs of the polymer coatings were also taken to show the variation of polymer deposition with the parameters studied.

Fourier transform infrared (FTIR) spectroscopy studies on a Nicolet 5DX were carried out on the deposited films through the following procedure: The film was scraped off the surface and dried at 60°C for 20 min, then 1.0 wt % of the material was mixed and ground with KBr and a pellet formed. The pellets were examined using FTIR spectroscopy. Full details are available in Desai.⁷

RESULTS AND DISCUSSION

Effect of Feeder Current

The experiments were carried out at constant feeder currents, ranging from 0.05 to 0.25 amp. A constant bed expansion of around 22.2% was used for these runs.

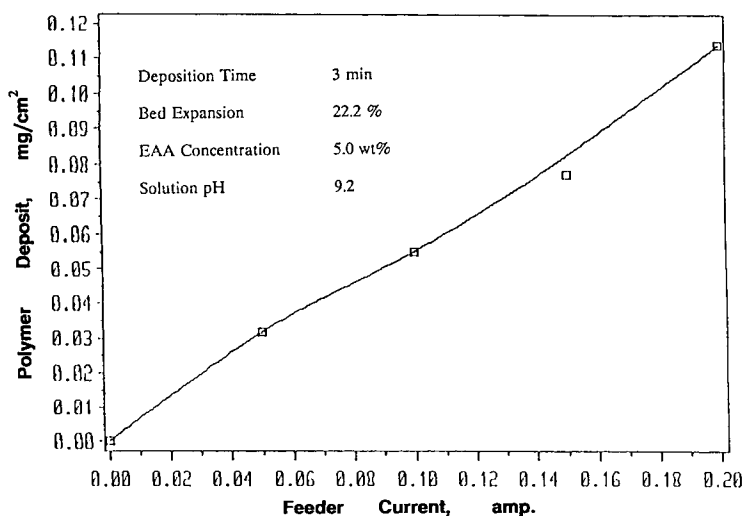


Figure 3 (a) Effect of feeder current on EAA polymer deposition.

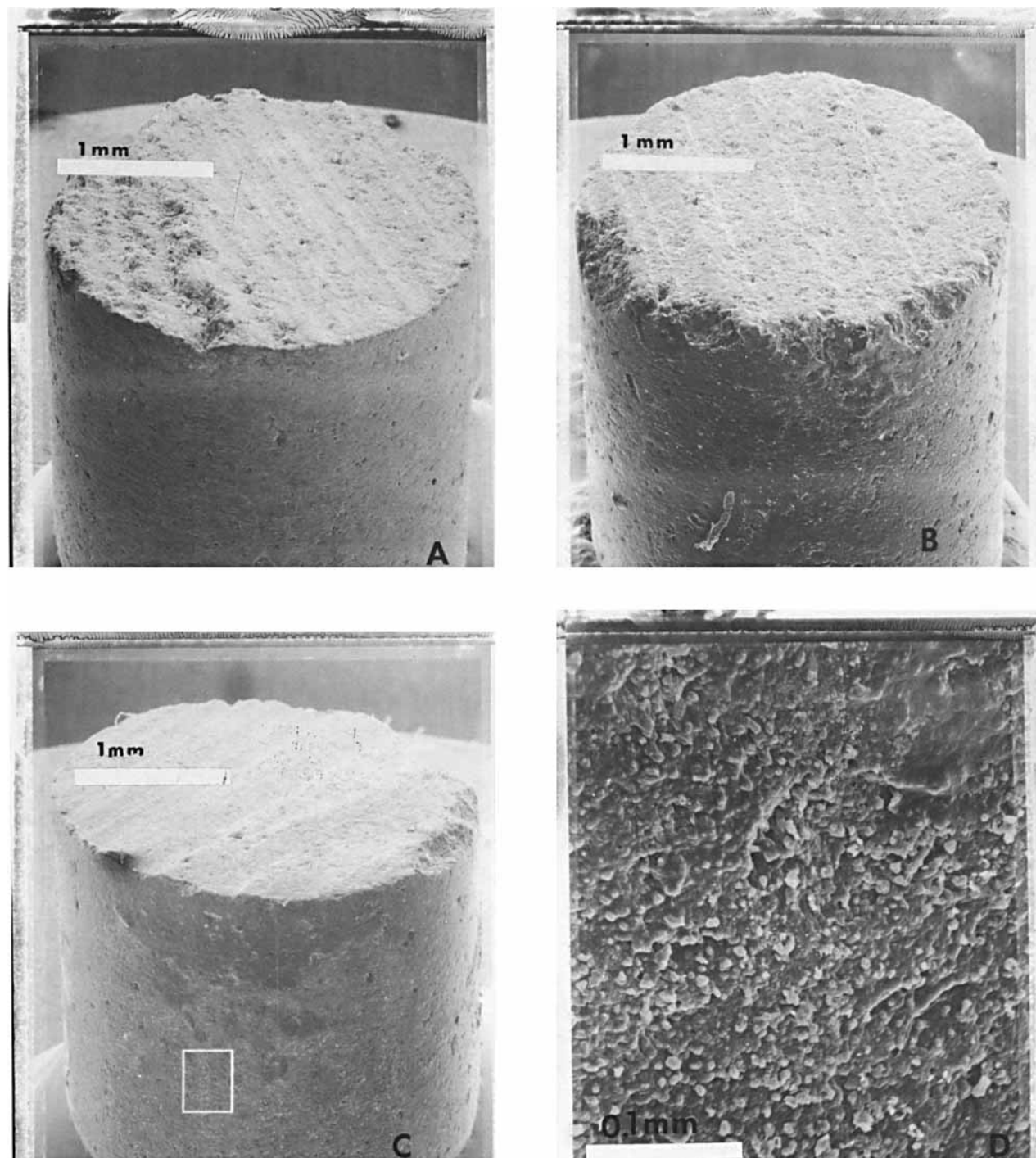


Figure 3 (b) SEM pictures showing effect of feeder current on EAA polymer deposition. (A) Feeder current: 0.05 amp, magnification 30 \times ; (B) feeder current: 0.10 amp, magnification 30 \times ; (C) feeder current: 0.15 amp, magnification 30 \times ; (D) feeder current: 0.15 amp, magnification 300 \times ; (E) feeder current: 0.20 amp, magnification 30 \times ; (F) feeder current: 0.20 amp, magnification 300 \times .

For a feeder current range of 0.1–0.2 amp, a deposition run time of 3 min was found to be feasible. In the case of a feeder current of 0.05 amp, the pro-

cess was halted after 3 min to enable appropriate polymer deposition comparison. For a feeder current of 0.25 amp, however, only 1 min of deposition was

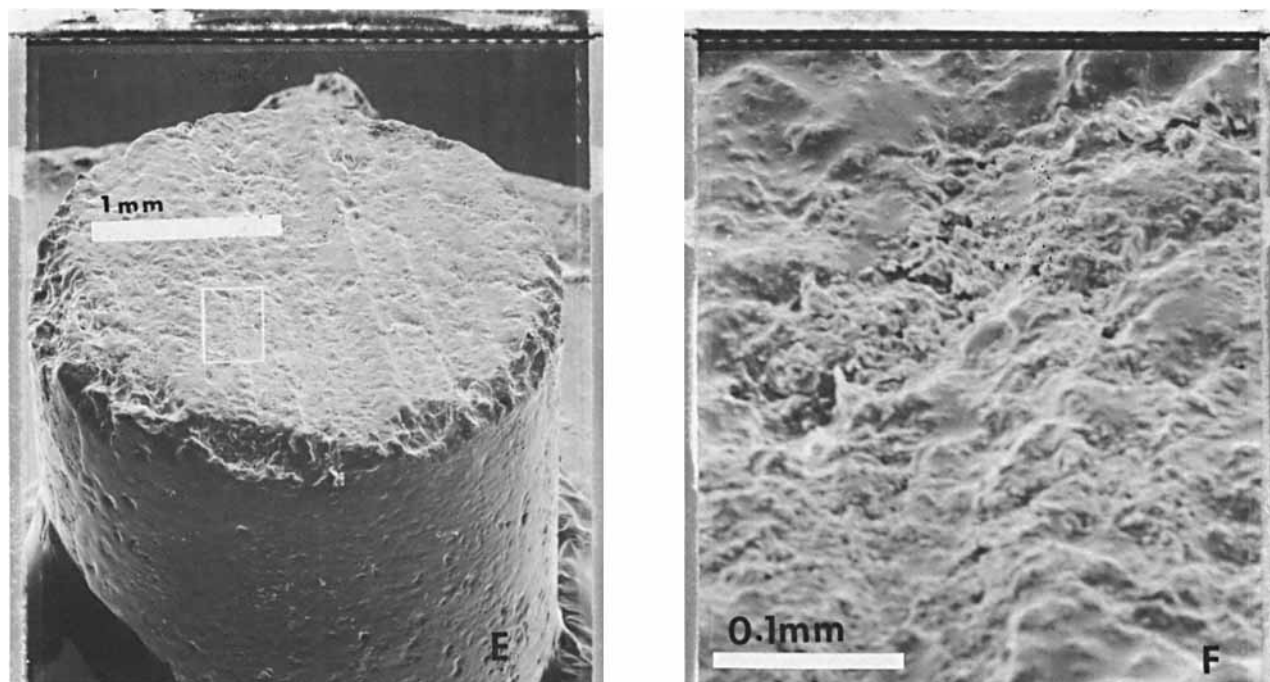


Figure 3 (Continued from the previous page)

possible. The limitation on run time was due to the nonconductive nature of the polymer deposit. The polymer films on the current feeder and the graphite particles decreased their conductivities, thus increasing the resistance to the flow of electrons. Hence, the voltage required to maintain the current constant had to be increased with time. For currents of 0.1 and 0.2 amp, it was possible to carry out the

process to an average approximate time of 3 min during which period the resistance of the cell was no doubt building up. After 3 min, the resistance of the cell had built up to such an extent that even a maximum applied voltage of 340 V could not support the current. At this point, the current began to decline rapidly and the run was terminated.

Figure 3(a) shows a plot of polymer deposition

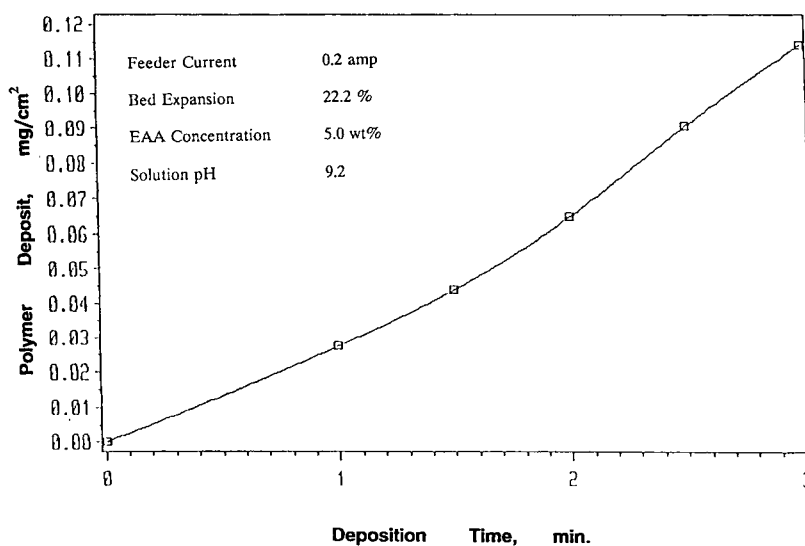


Figure 4 (a) Kinetics of EAA polymer deposition.

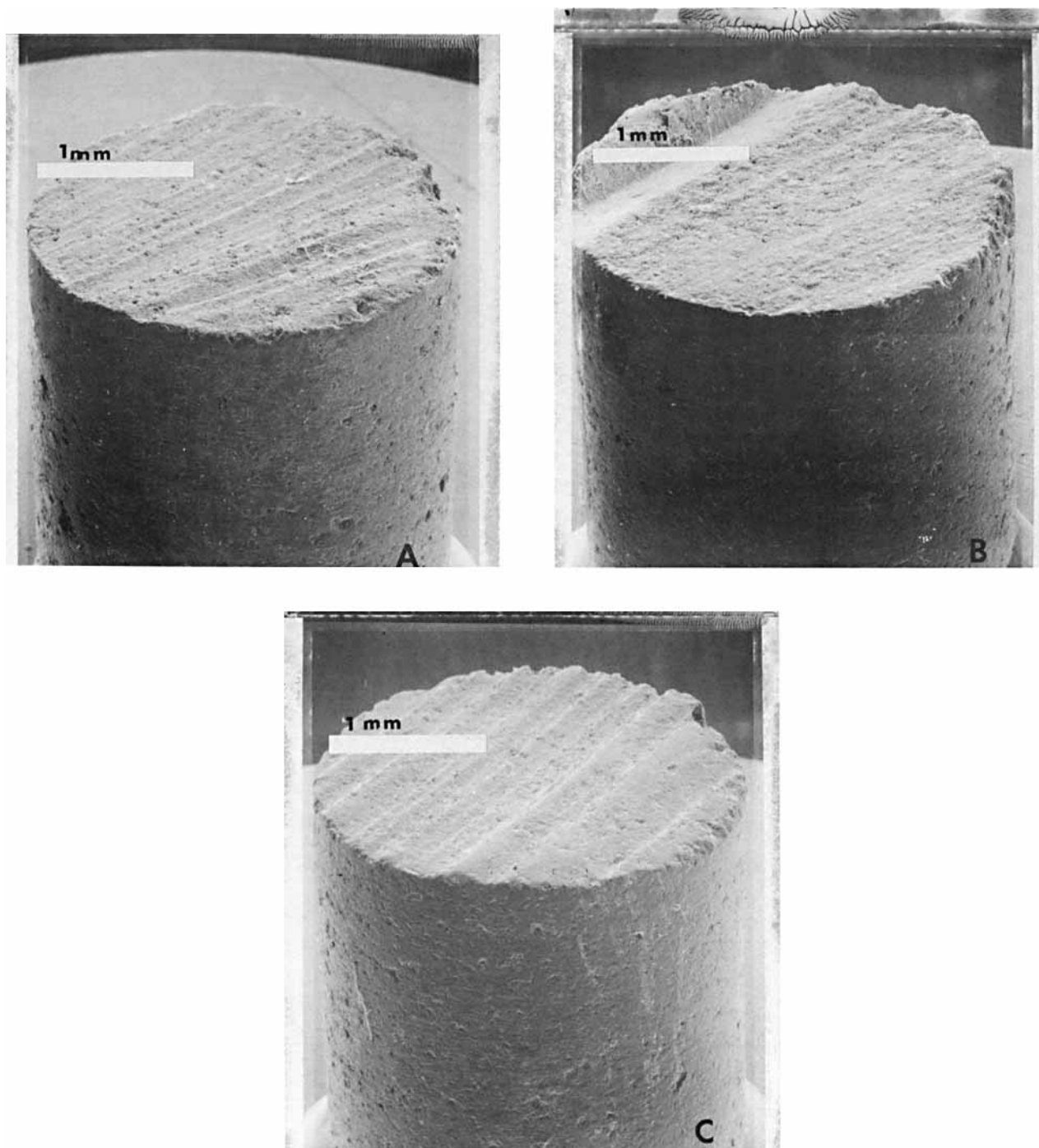


Figure 4 (b) SEM pictures on kinetics of EAA polymer deposition. (A) Time: 1.0 min, magnification 30 \times ; (B) time: 1.5 min, magnification 30 \times ; (C) time: 2.0 min, magnification 30 \times .

versus feeder current. The polymer deposition is highest at the feeder current of 0.2 amp. Hence, a feeder current of 0.2 amp was selected as optimum for all subsequent experiments.

The SEM pictures for film growth for various feeder currents are shown in Figure 3 (b). As can be seen, polymer deposition occurs for all feeder currents. For lower feeder currents, however, the film

is not so uniform, whereas at 0.2 amp, the entire particle is covered uniformly with a thin polymer film.

Effect of Deposition Time

The kinetics of film growth were next evaluated at the constant optimum feeder current of 0.2 amp described in the previous graph. The bed expansion was again maintained at 22.2%. Run time was varied from 1 to 3 min. Figure 4(a) shows the increase in polymer deposition with time. Figure 4(b) shows the corresponding SEM pictures. It is seen that there is no induction time and that polymer deposition occurs over the entire run time.

The approach of Rheineck and Usmani⁸ is applied to Figure 4(a) for EAA copolymer deposition. In the case of EAA, the polymer deposit appears to be always in the nucleation phase where it is a linear function of time. The diffusion-controlled growth phase normally seen after the initial nucleation phase is absent. This is further addressed in a later section, while considering the mechanism of electrodeposition of EAA. This deposition mechanism also has an effect on film morphology, and this also is addressed in that later section.

Effect of Anolyte Flow Rate

The variation of EAA polymer deposition with flow rate is shown in Figure 5. Two peaks were obtained: one at incipient fluidization and the other at around 22.2% bed expansion (bed porosity of 0.648). The observations in Figure 5 are explained as follows: When the bed is stationary, the entire surface area of the particles is not available for deposition. This

leads to lower polymer deposition values. As the flow rate is increased, more and more surface becomes available for polymer deposition through an increase in bed porosity, thus leading to increased polymer deposition. This trend is seen till incipient fluidization. At incipient fluidization, there is still no bed expansion but it is a point at which fluidization begins. At this point, practically the entire surface of the particles is available for deposition. Hence, the polymer deposition is maximum at this point.

The polymer deposition starts declining after this point. This is because, as the flow rate increases past the incipient fluidization state, the contact between the particles is broken. As the flow rate is increased further, both the mass transfer rates as well as the separation between particles increase. These two competing mechanisms have conflicting effects on polymer deposition, the former favoring an increase in polymer deposition and the latter favoring a decrease. In this region, at lower flow rates, however, the separation between the particles is not very high; thus, mass transfer effects predominate, leading to an increase in polymer deposition and giving rise to the second peak. This second peak is seen at a flow rate of 25 mL/s, i.e., at a bed expansion of around 22.5%. At higher flow rates, however, the separation between particles predominates, this again leading to a decrease in polymer deposition.

Mechanism for Electrodeposition of EAA

The mechanism for electrodeposition of EAA is illustrated in Figure 6. In aqueous ammonium solutions, EAA exists as ions. During electrolysis, pas-

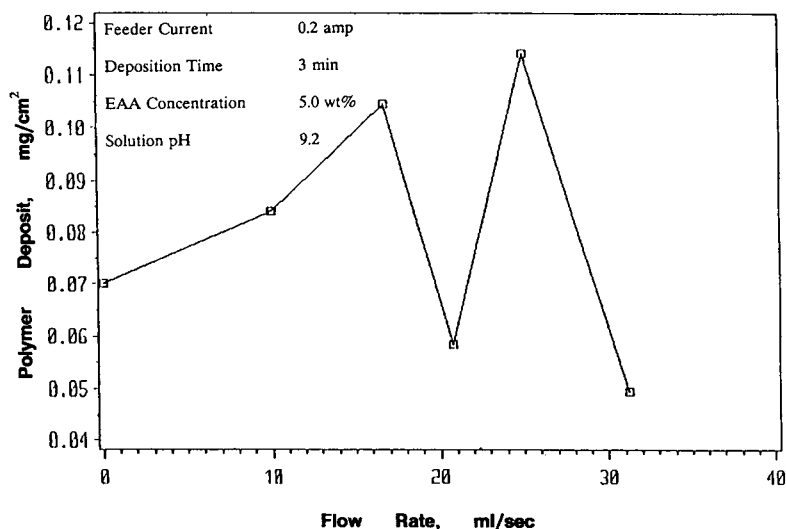


Figure 5 Effect of anolyte flow rate on EAA polymer deposition.

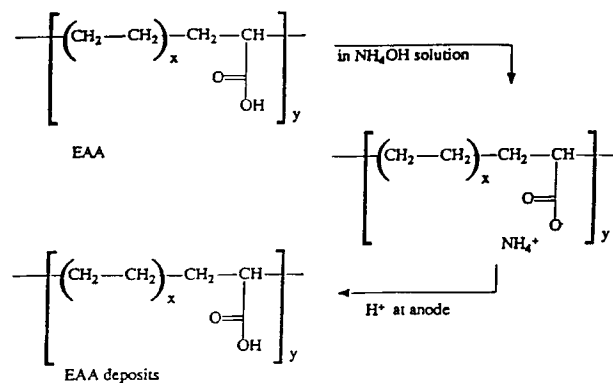


Figure 6 Mechanism of EAA polymer deposition.

sage of current through an electrode-solution interface causes chemical changes or migration of ions. When electrolysis begins, the hydrogen ion concentration in the immediate vicinity of the anode will be high. Because of this, the polymer forms an insoluble acid and precipitates out of the solution onto the surface of the anode. In EAA, however, there is only one carboxylic acid group and, hence, there is no elimination of water in the direct deposition of EAA as acid on the anode surface. As soon as the first layer of deposit is formed on the current feeder and on the graphite particles, the movement of hydrogen ions is restricted and can now occur only through the pores of the film. The EAA polymer, however, appears to have good film integrity; furthermore, since there is no elimination of water in the deposition mechanism, no cracks or pores are

seen in the film. Based on these, the film can be considered nonporous, and, hence, only a thin layer of film is produced, as no hydrogen ion transfer can occur after the formation of first layer of film. Thus, only a thin uniform film is seen in the case of EAA.

The kinetics of polymer deposition of EAA can now be examined in terms of an initial deposition phase and a subsequent growth phase. For EAA, only the first phase is seen where the polymer starts to form a monolayer on the particles and the complete coverage of the particles shows as an increase in polymer deposition with increase in time. The growth phase is, however, absent for EAA due to the nonporous nature of the film, as already explained.

Fourier Transform Infrared (FTIR) Spectroscopy

FTIR spectroscopic analyses were carried out on the deposited EAA films. Figure 7 shows a plot of % transmittance versus wave number for deposited EAA. It matches fairly well with the standard reference plot for EAA polymer.⁹ The band assignment^{10,11} is given in Table I.

CONCLUSIONS

The EAA films obtained were nonporous, continuous, and thin, with deposition only from the initially formed polymer. Thus, EAA films exhibit only the nucleation phase of deposition over the entire par-

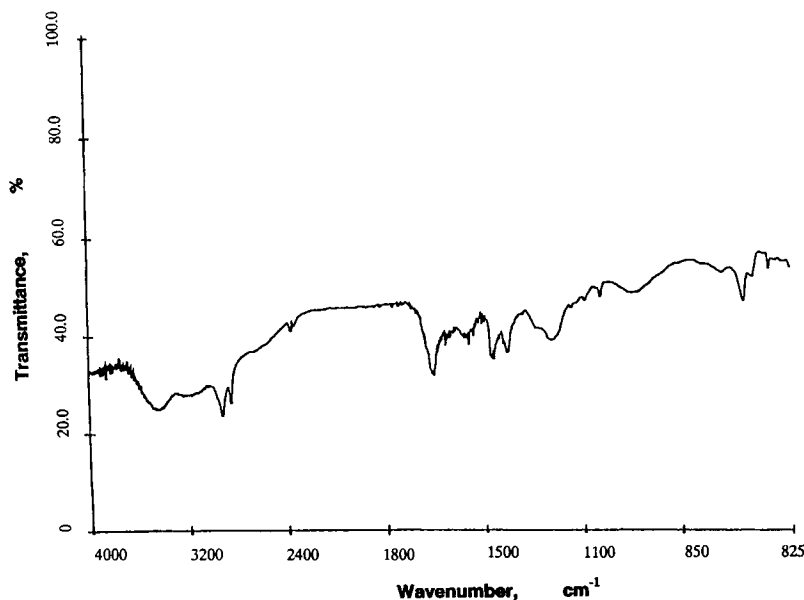


Figure 7 FTIR spectrum of EAA polymer.

Table I FTIR Band Assignments for EAA

No.	Band Wave Number (cm ⁻¹)	Possible Bond Assignment
1	2925	—CH ₂
2	2850	—CH
3	1650	—COOH
4	1530	—C=O
5	1470	—CH ₂
6	1400	—CH
7	1230	—C—OH
8	1060	—C—OH
9	970	—C—OH
10	715	—(CH ₂) _n

ticle surface. In the FEBR, the polymer film deposits were maximum at a feeder current of 0.2 amp and showed a dual-peak behavior with increasing anolyte flow rate. The peaks occurred at incipient fluidization and at approximately 22.2% bed expansion (i.e., at a bed porosity of 0.648). Since the EAA polymer film deposits were nonconductive, they allowed a maximum deposition time of only 3 min at 0.2 amp feeder current.

Portions of this research were supported with funds from the National Science Foundation Grant #CBT-8519001.

REFERENCES

1. R. Mahalingam, F. S. Teng, and R. V. Subramanian, *J. Appl. Polym. Sci.*, **22**, 3587 (1978).
2. F. S. Teng, Ph.D. Thesis, Chemical Engineering, Washington State University, Pullman, WA, 1979.
3. F. S. Teng and R. Mahalingam, *Polym. Commun.*, **27**, 342 (1986).
4. F. S. Teng and R. Mahalingam, *J. Appl. Polym. Sci.*, **34**, 2837 (1987).
5. S. Segelke, M.S. Thesis, Chemical Engineering, Washington State University, Pullman, WA, 1988.
6. S. Segelke, R. Mahalingam, and R. V. Subramanian, *J. Appl. Polym. Sci.*, **40**, 297 (1990).
7. V. M. Desai, M.S. Thesis, Chemical Engineering, Washington State University, Pullman, WA, 1988.
8. A. E. Rheineck and A. M. Usmani, *Electrodeposition of Coatings*, Adv. in Chem. Ser. 119, Am. Chem. Soc., Washington, DC, 1973.
9. C. J. Pouchert, *The Aldrich Library of Infrared Spectra*, 3rd Edition, Aldrich Chemical Co., Milwaukee, WI, 1981.
10. K. Nakanishi and P. H. Solomon, *Infrared Absorption Spectroscopy*, 2nd Edition, Holden-Day, Oakland, CA, 1977.
11. J. H. van der Maas, *Basic Infrared Spectroscopy*, 2nd Edition, Pitman Press, Aulander, NC, 1969.

Received March 12, 1990

Accepted October 16, 1990